Invited - Novel Microwave Devices and Structures Based on the Transmission Line Approach of Meta-Materials

Focused Session Paper

Christophe Caloz, and Tatsuo Itoh

Electrical Engineering Department, University of California, Los Angeles, CA, 90095, USA

Abstract — **This paper is composed of two parts. In the first part, the fundamentals of ideal transmission lines (TL) meta-materials (MM) with their physical characteristics and the synthesis of practical artificial TL-MMs with their circuital characteristics are presented. A microstrip implementation of a composite right / left handed (CRLH) TL is shown. In the second part, several novel applications based on the theory of the first part are demonstrated: a backfire-to-endfire leaky wave antenna, a coupled-line coupler with arbitrary coupling, a compact enhanced-bandwidth hybrid ring, a dual-band inharmonic branch-line coupler and a negative reflection / refraction phase-conjugating array interface.**

I. Introduction

In the last years, there has been significant interest for novel EM effects in meta-materials (materials with properties not existing in nature) and in particular for left-handed (LH) media (media in which the vectors $\boldsymbol{E}$, $\boldsymbol{H}$ and $\boldsymbol{k}$ form a LH triad) [1]-[8].

The TL approach of meta-materials recently introduced in [9]-[11] has paved the way for a novel class of devices and structures in the microwave domain.

This paper presents a generalized approach of MMs, considered in the general form of CRLH-TLs, and demonstrates several applications based on this approach.

II. Fundamentals of Ideal TL-MMs

The most general TL consists of the series combination of a conventional right-handed (RH) TL (low-pass) and its dual, the LH-TL (high-pass), forming a CRLH-TL (band-pass), as shown in Fig. 1. The fundamental physical characteristics of such a CRLH-TL can be derived from elementary TL theory and are summarized in Fig. 1. At low frequencies, the CRLH-TL is dominantly LH with the hyperbolic dispersive $\beta \approx \beta_L = -1/\omega\sqrt{L'_L C'_L}$, while at high frequencies, it is dominantly RH, with the linear non-dispersive $\beta \approx \beta_R = +\omega\sqrt{L'_R C'_R}$. The properties of the LH-TL derive from those of the RH-TL by low-pass to high-pass transformation, where the DC point is translated to infinity ($\omega \to 1/\omega$).

The transition frequency between the LH and RH ranges is given by $\omega_0 = \sqrt[4]{L'_L C'_L L'_R C'_R}$, $\beta_C(\omega_0) = 0$ and $\lambda_C(\omega_0) = \infty$. This follows from the fact that ω_0 corresponds to the center frequency of a band-pass filter and is therefore the image of DC. Matching is achieved by using L/C parameters in identical ratios in the RH and LH sections ($Z_0 = Z_{0R} = Z_{0L}$). Finally, the equivalent constitutive parameters ε, μ, n for a 2D/3D extension MM of the 1D-TL are obtained by comparing the immittances of a plane wave in an homogeneous medium with those of the TL. In a LH medium, these parameters are negative and dispersive, but satisfy the general entropy conditions for dispersive media.

Fig. 2 shows the dispersion diagram of a CRLH-TL, which may include four distinct regions in the case of an open structure: LH-guided, LH-leaky, RH-leaky and RH-guided. At the transition frequency ω_0, the LH and RH contributions exactly compensate each other ($\beta_L = -\beta_R$), which leads to the infinitely fast-wave $\beta_C = 0$. If the RH contribution is progressively reduced to zero ($L'_R, C'_R \to 0$), regions IV and then III disappear, and eventually the CRLH curve collapses to the pure LH curve.

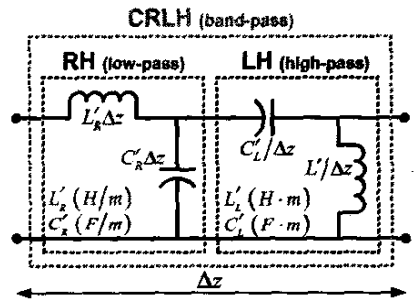

- $\beta_C = \beta_R + \beta_L$
  with $\beta_R = \omega/\omega_R$ $\beta_L = -\omega_L/\omega$
  and $\omega_R = 1/\sqrt{L'_R C'_R}$ $\omega_L = 1/\sqrt{L'_L C'_L}$
- transition: $\beta_C(\omega_0) = 0$, $\omega_0 = 1/\sqrt[4]{L'_R C'_R L'_L C'_L}$
- $\lambda_C = 2\pi/|\beta_C| = 2\pi/|\omega/\omega_R - \omega_L/\omega|$, $\lambda_C(\omega_0) = \infty$
- $v_{pC} = \omega/\beta_C = \omega/[\omega/\omega_R - \omega_L/\omega]$
- $v_{gC} = (d\beta_C/\omega)^{-1} = \left[1/\omega_R + \omega_L/\omega^2\right]^{-1}$
- $Z_{0R} = Z_{0L}$ (matching)
  with $Z_{0R} = \sqrt{L'_R/C'_R}$ $Z_{0L} = \sqrt{L'_L/C'_L}$
- $\varepsilon_{rR} = C'_R$, $\mu_{rR} = L'_R$, $n_R = \sqrt{L'_R C'_R}$
- $\varepsilon_{rL} = -1/\omega^2 L'_L$, $\mu_{rL} = -1/\omega^2 C'_L$, $n_L = -c_0/\omega^2\sqrt{L'_L C'_L}$
- $n_C = n_R + n_L$

Fig. 1. Ideal CRLH-TL. Equivalent circuit for an incremental length of (lossless) CRLH-TL with corresponding physical parameters: propagation constant β, transition frequency ω_0, guided wavelength λ, phase/group velocities v_p/v_g, characteristic impedance Z_0, equivalent permittivity ε, permeability μ and refractive index n. The indexes R, L, C refer to RH, LH and CRLH, respectively.

0-7803-7695-1/03/$17.00 © 2003 IEEE

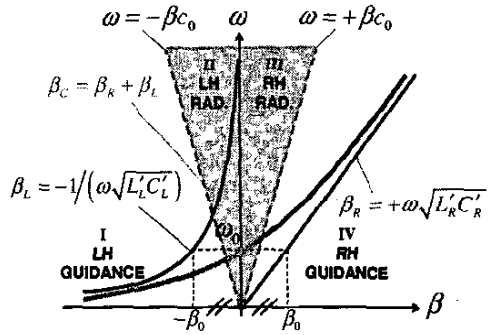

Fig. 2. Dispersion diagram for the ideal CRLH-TL of Fig. 1. The curves $\omega=\pm\beta c_0$ represent the air lines: if $\omega>|\beta c_0|$ (shaded area) and the structure is open in the direction y perpendicular to the direction of the line, then $k_y=\sqrt{\omega^2-(\beta c_0)^2}$ is real in the fields dependence $\exp(-jk_y y)$ and leakage/radiation occurs.

III. Synthesis of Practical Artificial TL-MMs

Although the RH-TL represents conventional lines and physical materials used in practice, the ideal LH-TL does not exist in nature. However, an artificial lumped-element (LE) implementation of such a line, or more generally of a CRLH-TL, is possible in the form a ladder-network, obtained by repeating periodically an appropriate unit-cell circuit. The general synthesis of a LE artificial CRLH-TL is described in Fig. 3, where the different formulas can be derived by elementary circuit theory. While the ideal TLs presented in Sec. II are transmitting from DC to ∞, their LE implementations include stop-bands, and are valid only in their pass-bands. To increase their bandwidth, it is necessary to increase the number of unit-cells N and to adjust consequently the values of the L/C elements according to the formulas given in Fig. 3 in order to keep the electrical characteristics of the line unchanged. An essential condition for the LE approximation of an ideal TL to be possible is that the electrical length of the unit-cell ϕ_C be small enough ($\phi_C<\pi/2$) to ensure that the unit-cell shown in Fig. 3 can be a reasonable approximation of the infinitesimal circuit model of Fig. 1.

A distributed quasi-lumped microstrip implementation of a CRLH-TL is shown in Fig. 4, where left-handedness is obtained below the transition frequency f_0=3.9 GHz. When frequency is increased above f_0, the interdigital capacitors are not quasi-lumped any more, and eventually resonate with their parasitic series inductance (at around 5.5 GHz). Also, in this implementation the inductance changes also as $Z_0\tan(\theta_{stub})/\omega$, and eventually becomes capacitive. However, both the LH and RH effects obtained below and above ω_0, respectively, can be exploited in practical applications.

The evolution of the guided wavelength predicted in Fig. 1 (λ_C increasing from 1.5 GHz to 3.9 GHz, infinite at 3.9 GHz, and decreasing above) could be clearly observed in the animated field distributions of full-wave simulations (Ansoft-Ensemble and Sonnet-em).

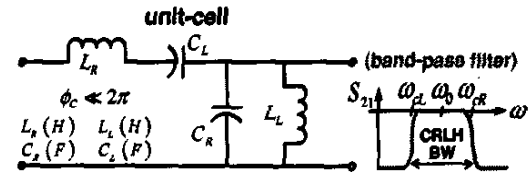

- $\omega_{cL}=\omega_{0L}/2$ $\omega_0=\sqrt{\omega_{0R}\omega_{0L}}$ $\omega_{cR}=2\omega_{0R}$ (∞ periodic)
  with $\omega_{0R}=1/\sqrt{L_RC_R}$ $\omega_{0L}=1/\sqrt{L_LC_L}$
- $Z_{0R}=Z_{0L}$ (matching), with $Z_{0R}=\sqrt{L_R/C_R}$, $Z_{0L}=\sqrt{L_L/C_L}$
- $\phi_C=\phi_R+\phi_L$ (unit-cell)
  with $\phi_R=-\arctan\left[\omega\kappa_R/\left(2-(\omega/\omega_{0R})^2\right)\right]<0$: lag
  and $\phi_L=-\arctan\left[\omega\kappa_L/\left(1-2(\omega/\omega_{0L})^2\right)\right]>0$: advance
  and $\kappa_R=L_R/Z_{0R}+C_RZ_{0R}$ $\kappa_L=L_L/Z_{0L}+C_LZ_{0L}$
- $t_{gC}=t_{gR}+t_{gL}$ (unit-cell)
  with $t_{gR}=\kappa_R\left[2+(\omega/\omega_{0R})^2\right]\Big/\left\{\kappa_R^2\omega^2+\left[2-(\omega/\omega_{0R})^2\right]^2\right\}$
  and $t_{gL}=\kappa_L\left[1+2(\omega/\omega_{0L})^2\right]\Big/\left\{\kappa_L^2\omega^2+\left[1-2(\omega/\omega_{0L})^2\right]^2\right\}$
- approximation of line of length p with N unit-cells:
  $C_R=C_R'\cdot(p/N)$ $L_R=L_R'\cdot(p/N)$
  $C_L=C_L'\cdot(N/p)$ $L_L=L_L'\cdot(N/p)$
  $\Big\}$ $\left\{C_R',L_R',C_L',L_L'\right.$ fct of line implementation
  → homogeneity/isotropy condition: $\phi_C<\pi/2$
- $\phi_C^{tot}=N\cdot\phi_C$, $t_{gC}^{tot}=N\cdot t_{gC}$

Fig. 3. LE implementation of an artificial CRLH-TL. Unit-cell circuit with corresponding circuital parameters: cutoff frequencies ω_c, transition frequency ω_0, characteristic impedance Z_0, unit-cell phase shift ϕ and group delay t_g, components values for the complete ladder-network implementation of the TL.

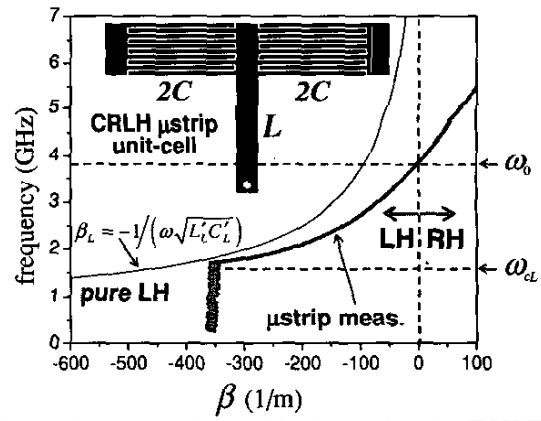

Fig. 4. Microstrip quasi-lumped implementation of a CRLH-TL (high-pass filter). Measured dispersion curve obtained by unwrapping the phase of S_{21} for a 7-unit-cells microstrip CRLH-TL. The unit-cell constituted of two series interdigital capacitances and one shunt shorted stub inductor is shown in the inset ($2C$=2.4pF and L=6.5nH @ 3GHz). The substrate is the RT/Duroid 5880 (ε_r=2.2, h=62 mils).

IV. Applications

A. Backfire-to-Endfire Leaky-Wave Antenna [12]

The backfire-to-endfire leaky-wave antenna is a direct application of the concept of open CRLH-TL described in

Fig. 2. Radiation patterns for the antenna consisting of the same microstrip line as that of Fig. 4, terminated by a matched load, are shown in Fig. 5. They demonstrate that the antenna, operated in its fundamental mode, can be scanned both backward (LH) and forward (RH) with broadside radiation at the transition frequency f_0. Measurements revealed that the antenna can be scanned from backfire to endire in the range from *3.1* to *6.0* GHz.

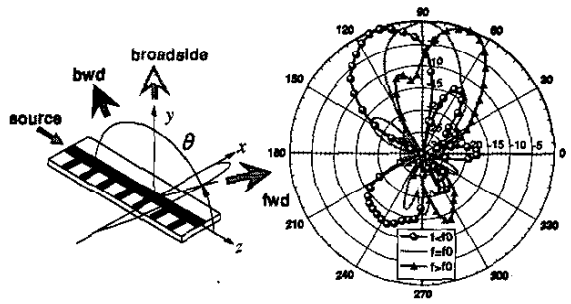

Fig. 5. Backfire-to-endfire leaky-wave antenna and radiation patterns at frequencies located in the LH region $f<f_0$ (backward), at the transition frequency $f=f_0=3.9$ GHz (broadside) and in the RH region $f>f_0$ (forward) (see Fig. 2).

B. Coupled-Line Coupler with Arbitrary Coupling

Combining a LH-TL, such as that of Fig. 4, with a conventional RH-TL into a coupled-line coupler leads to a backward coupler operating as an (enhanced) forward coupler (coupling increasing with the electrical length l_e [13]). This coupler is capable of virtually any loose/tight coupling level, as illustrated in Fig. 6, where *0*-dB coupling is achieved over more than *35%* bandwidth. Coupling rapidly increases to reach *0*-dB as frequency is decreased below f_0 because l_e increases when ω decreases ($l_e = l/\lambda \propto 1/\omega$) in the LH range. A symmetric (quadrature) LH/LH coupler, providing similar performances was also investigated, and observed to be based on both magnetic and electric coupling phenomena, very different from those occurring conventional couplers.

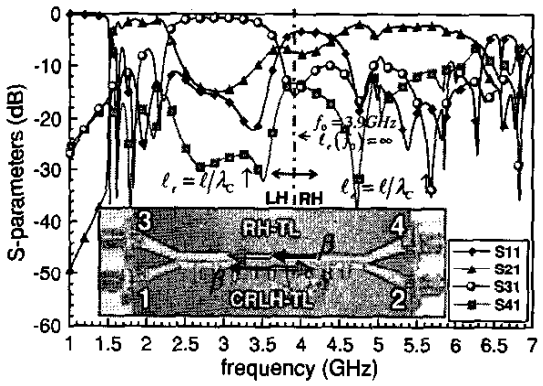

Fig. 6. Measured performances of the RH-LH quasi-*0*-dB coupled-line backward coupler with spacing $s=0.3$mm ($s/h=0.19$). The transition frequency is $f_0=3.9$ GHz. β and S represent the propagation constant and the Poynting vector, respectively, in each of the two lines. The same s/h provides less then *-10*-dB coupling in the conventional case.

C. Compact Enhanced-Bandwidth Hybrid Ring

A compact enhanced-bandwidth hybrid ring is obtained by replacing the *270°* RH line section of the conventional rat-race by a *-90°* CRLH-TL, which exhibits a much milder frequency dependence, as it can be seen in Fig. 2. The hybrid realized, shown in Fig. 7, uses a *-90°* CRLH-TL composed of three SMT chip components LH *C/L* cells (*-3x35°*) and three short interconnecting microstrip lines (*+3x5°*). The insertion loss results in Fig. 7 show a *54%* bandwidth enhancement and *67%* size reduction compared to the conventional hybrid at 2 GHz.

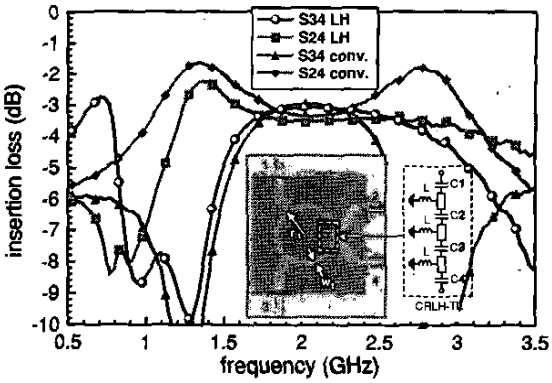

Fig. 7. Measured insertion losses of the enhanced-bandwidth hybrid ring compared to those of the conventional hybrid ring.

D. Dual-Band Non-harmonic Branch-Line Coupler

The conventional branch-line coupler is characterized by the periodic repetition of its spectrum at odd harmonics of the design frequency. Replacing the branches-lines by CRLH-TLs, as shown in the prototype of Fig. 8 increases the versatility of the component by making two arbitrary operating frequencies available. The underlying principle can be understood from Fig. 2: the additional degree of freedom provided by the DC-offset due to the LH contribution allows an arbitrary pair of frequencies (at *90°* and *270°*) to be intercepted by the phase curve of the CRLH-TL. The performances of the fabricated component are shown in Fig. 8.

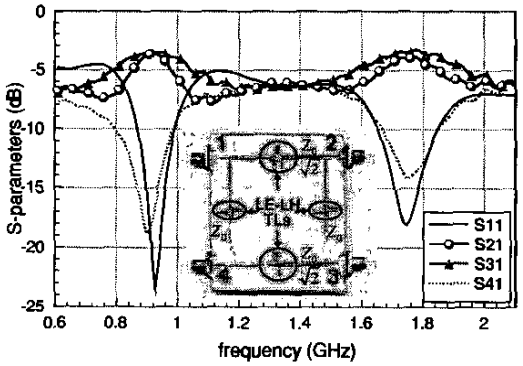

Fig. 8. Measured performances of the dual-band inharmonic branch-line coupler. The design frequencies are *920* MHz and *1740* MHz, respectively.

E. Negative "Reflective/Refractive" Phase-Conjugating Antenna Array Meta-Interface

The concept of "meta-interface", concentrating RH/LH interface effects within a thin interface and thereby avoiding losses and dispersion inherent to an artificial LH-MM, is approached in the negative "reflection/refraction" structure described in Fig. 9. The incident (RF) wave is reflected (IF) backward to the source after phase-conjugation (phase inversion of incoming RF with LO-freq = 2× RF-freq at each element) realized by Schottky diode mixers, which may be interpreted as negative reflection. More interestingly, half of the IF signal is re-radiated on the other side of the substrate with a negative-refractive-like angle due to the use of bidirectional slot antenna elements. These effects are illustrated in Fig. 9 for the case of a 30^{o} incoming angle. Near-field focusing effects were also observed.

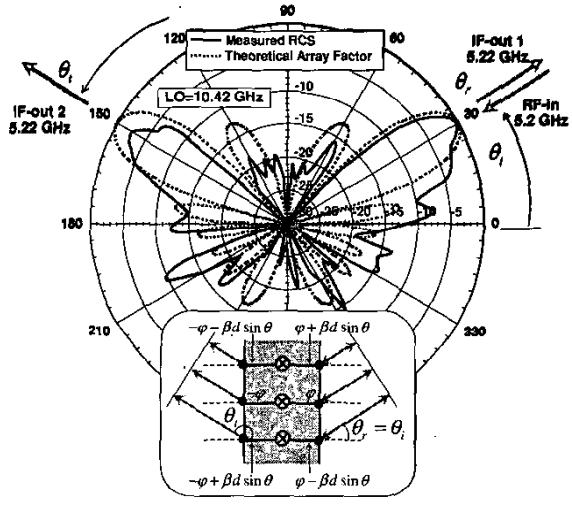

Fig. 9. Working principle and measured far-field patterns of the negative reflection/refraction phase-conjugating meta-interface.

V. Conclusion

The TL approach of MMs, considered in general as CRLH-TLs, was summarized. The fundamental characteristics and equations for both the ideal CRLH-TL and the artificial LE-circuit implementation of this line were presented. Several microwave applications, including novel components, antenna and surface/interface were demonstrated. It is expected that the new concepts associated with TL-MMs will lead to the development of materials and structures with unprecedented properties in the coming years.

Acknowledgement

This work is part of the MURI program "Scalable and Reconfigurable Electromagnetic Metamaterials and Devices". It was supported by the Department of Defense (N00014-01-1-0803) and monitored by the U.S. Navy/Office of Naval Research.

References

[1] L. J. Wang, A. Kuzmich, and A. Dogariu, "Gain-Assisted Superluminal Light Propagation," *Nature*, vol. 406, pp. 277-278, July 2000.

[2] R. W. Ziolkowski, "Superluminal Transmission of Information Through an Electromagnetic Metamaterial," *Phys. Rev. E*, vol. 63-046604, pp. 1-13, 2001.

[3] J. B. Pendry, A. J. Holden, D. J. Robbins, and W. J. Stewart, "Magnetism from Conductors and Enhanced Nonlinear Phenomena," *IEEE Trans. Microwave Theory and Tech*, vol. 47, no. 11, pp. 2075-2084, Nov. 1999.

[4] M. Notomi, "Theory of Light Propagation in Strongly Modulated Photonic Crystals: Refraction like Behavior in the Vicinity of the Photonic Band Gap," *Phys. Rev. B*, vol. 62, no. 16, pp. 10696-10705, Oct. 2000.

[5] V. G. Veselago, "The Electrodynamics of Substances with Simultaneously Negative Values of ε and μ," *Soviet Physics Uspekhi*, vol. 10, no. 4, pp. 509-514, Jan.-Feb. 1968.

[6] D. R. Smith, W. J. Padilla, D. C. Vier, S. C. Nemat-Nasser, and S. Schultz, "Composite Medium with Simultaneously Negative Permeability and Permittivity," *Phys. Rev. Lett.*, vol. 84, no. 18, pp. 4184-4187, May 2000.

[7] J. B. Pendry, "Negative Refraction Makes a Perfect Lens," *Phys. Rev. Lett.*, vol. 85, no. 28, Oct. 2000.

[8] R. A. Shelby, D. R. Smith, and S. Schultz, "Experimental Verification of a Negative Index of Refraction," *Science*, vol. 292, pp. 77-79, Apr. 2001.

[9] C. Caloz, H. Okabe, T. Iwai, and T. Itoh, "Transmission Line Approach of Left-Handed (LH) Materials," *USNC/URSI National Radio Science Meeting*, vol. 1, p. 39, San Antonio, TX, June 2002.

[10] C. Caloz, and T. Itoh, "Application of the Transmission Line Theory of Left-Handed (LH) Materials to the Realization of a Microstrip LH Transmission Line," *IEEE-APS Int'l Symp.*, vol. 1, pp. 412-415, San Antonio, TX, June 2002.

[11] A. K. Iyer, and G. V. Eleftheriades, "Negative Refractive Index Metamaterials Supporting 2-D Waves," *IEEE-MTTInt'l Symp.*, pp. 1067-1070, Seattle, WA, June 2002.

[12] L. Liu, C. Caloz, and T. Itoh, "Dominant Mode (DM) Leaky wave Antenna with Backfire-to-Endfire Scanning Capability," *Electron. Lett.*, vol. 38, no. 23, pp. 1414-1416, Nov. 2002.

[13] R. Mongia, I. Bahl and P. Bhartia, *RF and Microwave Coupled-Line Circuits*. Norwood, MA: Artech House, 1999.